High-rate Viscoelastic Shear Model of Porcine Skin, Lung and Liver Tissue

Joost Op 't Eynde, Christopher P. Eckersley, Cameron R. Bass

Injury Biomechanics Laboratory, Department of Biomedical Engineering, Duke University, Durham, NC, USA

Introduction

- Ballistic body armor provides protection to both civilian and military victims of high velocity gunshot wounds to the chest and abdomen, reducing both mortality rates and injury severity.
- Body armor stops an incoming round by deforming, resulting in backface deformation that can cause local injuries in the underlying tissues. This is often called Behind Armor Blunt Trauma (BABT).
- Finite element models are often used as a tool to study BABT injuries, relying on accurate material properties of not only the skeletal structure, but also local soft tissue properties.
- To accurately represent biological soft tissues, their viscoelastic relaxation behavior must be accounted for.
- Compression and tension testing of skin and liver has been studied in literature but shear strength, an important component in BABT, has not often been a focus of study.
- Porcine skin and organs have been used as a surrogate for human skin and organs because they have similar mechanical properties, and there are histological and biochemical similarities.
- Plastilina clay is a poor surrogate for human tissues in BABT testing. Ballistic gelatin has been used as well.
- We characterize the viscoelastic shear properties of porcine skin, lung, and liver tissue, and compare them to the shear properties of synthetic ballistic gelatin. These properties can serve as a first approximation for human tissue properties.

Shear Test Setup

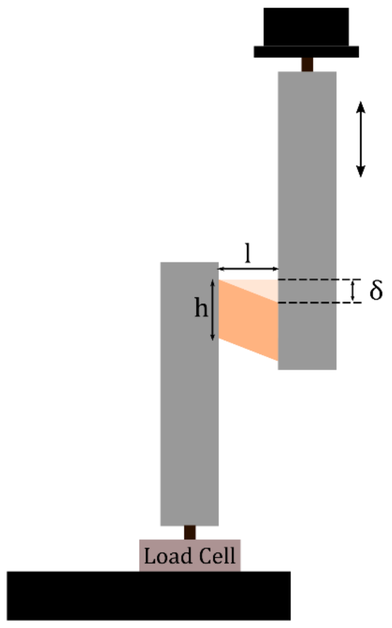

Figure 1:
Shear test setup schematic.

Shear Testing

- Porcine lung, liver, dorsal and ventral skin was obtained immediately post mortem and stored in saline at 4 °C. Before testing, tissue was cut into 10x10x10 mm cubes, or to thickness of the skin. Synthetic gelatin (10% and 20%, Clear Ballistics ®) was heated and molded into the same size cubes.
- Specimens were attached to two metal plates (Figure 1) with a sandpaper surface using cyanoacrylate glue, and tested in an orientation transverse to the organ surface. For each tissue type, 5 specimens were tested at room temperature.
- Each specimen was tested at shear strain levels of 10%, 15%, 30% and 40%, with a high-rate ramp (~ 100 s^{-1}) followed by a 100 s hold to examine viscoelastic relaxation, repeated 3 times.
- Force F and displacement δ were recorded and converted to shear stress τ and shear strain γ $\quad \tau = \frac{F}{A} = \frac{F}{h \cdot w} \qquad \gamma = \frac{\delta}{l}$ (Figure 1)

Viscoelastic Modeling

- To characterize the viscoelastic properties of the tested tissues, quasilinear viscoelastic behavior was assumed, and shear stress was modeled using the hereditary integral:

$$\tau_M(\gamma, t) = \int_0^t R(t - t') \frac{d\tau_{el}(\gamma(t'))}{dt'} dt'$$

with generalized Maxwell reduced relaxation function

$$R(t) = R_\infty + \sum_{i=1}^{n} R_i e^{-\beta_i t} \quad with \quad R_\infty + \sum_{i=1}^{n} R_i = 1$$

and instantaneous elastic function modeled linear or exponential

$$\tau_{el} = G \cdot \gamma \quad \text{or} \quad \tau_{el} = A(e^{B\gamma} - 1)$$

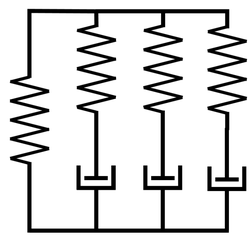

Figure 2: Generalized Maxwell Model.

- After initial optimization, three terms were chosen for the relaxation function, with fixed time constants ($1/\beta$) of 20 s, 1 s, and 10 ms.
- The viscoelastic model was optimized for instantaneous elastic parameters G or A and B, and relaxation parameters R_∞ and R_i, and these parameters were used to compare across tissues.

Results

- Tissues were found to have exponential stress-strain behavior at higher shear strain levels (30-40%), while being mostly linear at lower shear strain levels (10-15%). The exponential form of the instantaneous relaxation function improved the model fit sum squared error by an average of 8.6%. We recommend that any computational models include non-linear shear behavior. However, as both A and B can vary across tissues, the linear instantaneous elastic function was used for ease of comparison.

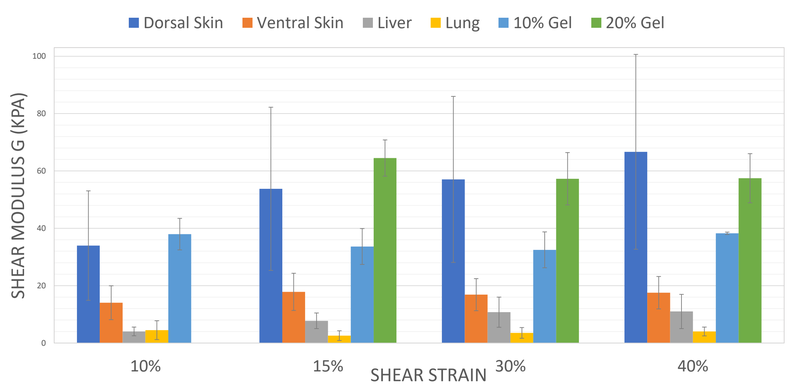

Figure 3: Linear shear modulus G for each tissue at each strain level (±SD).

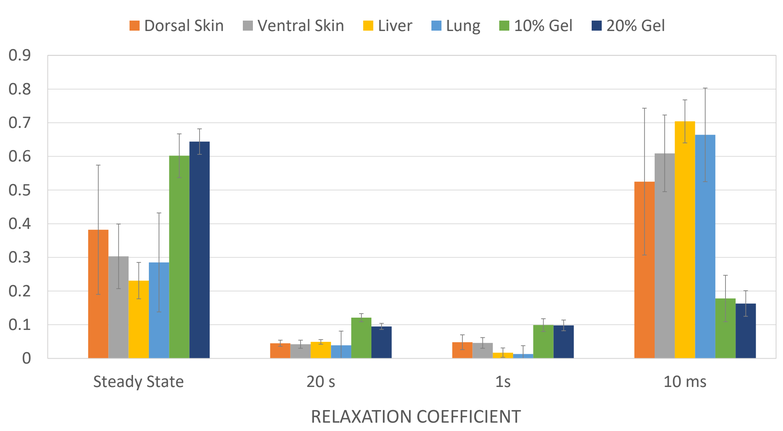

Figure 4: Viscoelastic relaxation coefficients for 30% shear strain test (±SD).

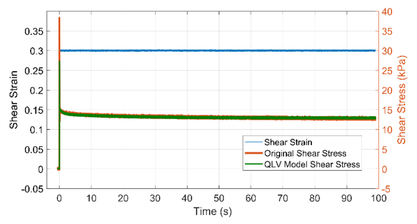

Figure 5: Dorsal skin 30% shear measurements and model.

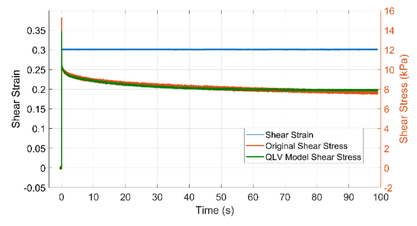

Figure 6: 10% gelatin 30% shear measurements and model.

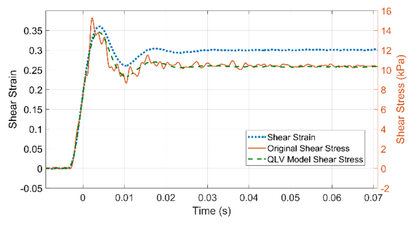

Figure 7: 10% gelatin 30% shear measurements and model results from Figure 6 at short time scale.

Discussion

- The instantaneous elastic model parameters can be found in Figure 3. The dorsal skin had the highest shear strength of all the tissues, followed by the ventral skin and then the liver and lungs. The reported values exceed those reported in literature for low-rate loading, but fall below shear moduli reported in split-Hopkinson bar experiments.
- The 20% ballistic gelatin was comparable to dorsal skin in shear strength, and the 10% gelatin had lower shear strength, but still significantly higher than the other tissues. Viscoelastic relaxation coefficient of the biological tissues are dramatically different from the ballistic gelatin, with the biological tissues relaxing over a much shorter time scale, and relaxing more overall.
- Future studies will include an evaluation of frozen and thawed tissue properties, and the effects of environmental temperature, as well a parallel orientation for shear testing.

Conclusions

- A quasilinear viscoelastic model was applied to high-rate high amplitude shear in porcine skin, liver and lungs, and provided good fit. These material properties provide a first approximation for the properties of human tissues.
- Shear moduli increase at higher strain levels for porcine tissues, suggesting non-linear elastic behavior.
- Synthetic ballistic gelatin (20%) provides a good shear stiffness approximation for dorsal porcine skin, but the relaxation behavior is different.
- Porcine dorsal and ventral skin have significantly different shear stiffness, and will need to be compared to human skin to determine an appropriate surrogate.

Acknowledgements & References

The authors gratefully acknowledge the funding and collaboration from MTEC-18-04-I-PREDICT-07, Incapacitation Prediction for Readiness in Expeditionary Domains, an Integrated Computational Tool (I-PREDICT) Thorax Model Prototype.

1. Bass, CR. et al. (2006). *Int J Occup Saf Ergo, 12*(4), 429-442.
2. Peleg, K. et al. (2006). *J Am Coll Surgeons, 202*(4), 643-648.
3. Latourette, T. (2010). *J Occup Environ Hyg, 7*(10), 557-562.
4. Fung, YC. (2013). Biomechanics: mechanical properties of living tissues. *Springer Science & Business Media.*
5. Edwards, C. et al. (1995). *Clin Dermatol*, *13*(4), 375-380.
6. Shergold, OA. et al.(2006). *Int J Impact Eng, 32*(9), 1384-1402.
7. Hanlon, E. et al. (2012). *Mil Med, 38*(5), 576-584.
8. Lamers, E. et al. (2013). *J Mech Behav Biomed, 28*, 462-470.
9. Saraf, H. et al. (2007). *J Biomech, 40*(9), 1960-1967.
10. Liu, Z. et al. (2002). *Biorheology, 39*(6), 735-742.